Short Article

Cell Metabolism

Mitochondrial ROS Produced via Reverse Electron Transport Extend Animal Lifespan

Graphical Abstract

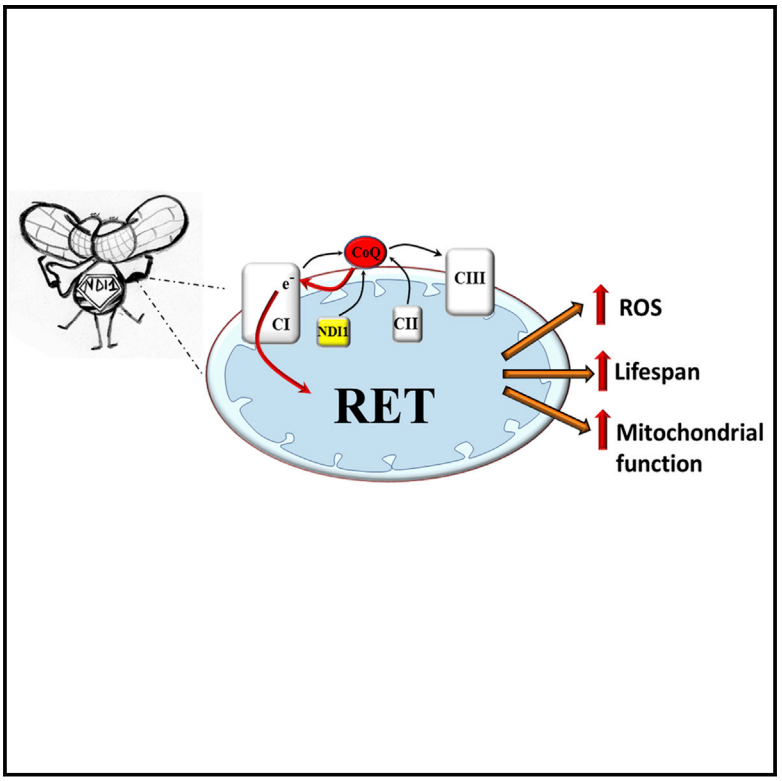

Authors

Filippo Scialò, Ashwin Sriram, Daniel Fernández-Ayala, ..., Jose Antonio Enríquez, Michael P. Murphy, Alberto Sanz

Correspondence

Alberto.Sanz@newcastle.ac.uk

In Brief

Increasing mitochondrial ROS (mtROS) specifically through complex I improves health and extends lifespan. Scialò et al. show that the site at which mtROS are produced determines their effects and increasing mtROS specifically via reverse electron transport through mitochondrial complex I delays aging and the onset of age-related diseases in flies.

Highlights

- Mitochondrial ROS accumulate in the fly brain during aging
- Inducing reverse electron transport (RET) in vivo increases mitochondrial ROS
- RET extends fly lifespan through a ROS-mediated mechanism
- RET improves mitochondrial function in a model of Parkinson's disease

Scialò et al., 2016, Cell Metabolism *23*, 725–734
April 12, 2016 ©2016 The Authors
http://dx.doi.org/10.1016/j.cmet.2016.03.009

CellPress

Cell Metabolism
Short Article

Mitochondrial ROS Produced via Reverse Electron Transport Extend Animal Lifespan

Filippo Scialò,[1,7] Ashwin Sriram,[1,7] Daniel Fernández-Ayala,[2] Nina Gubina,[3] Madis Lõhmus,[4] Glyn Nelson,[1] Angela Logan,[5] Helen M. Cooper,[4] Plácido Navas,[2] Jose Antonio Enríquez,[6] Michael P. Murphy,[5] and Alberto Sanz[1,*]
[1]Institute for Cell and Molecular Biosciences, Newcastle University Institute for Ageing, Newcastle University, Newcastle upon Tyne NE4 5PL, UK
[2]Centro Andaluz de Biología del Desarrollo, Universidad Pablo de Olavide-CSIC, and CIBERER, ISCIII, Seville 41013, Spain
[3]The Institute of Theoretical and Experimental Biophysics RAS, Pushchino 142290, Russia
[4]Department of Biosciences, Åbo Akademi University, Turku FI-20520, Finland
[5]MRC Mitochondrial Biology Unit, Hills Road, Cambridge CB2 0XY, UK
[6]Centro Nacional de Investigaciones Cardiovasculares Carlos III (CNIC), Melchor Fernández Almagro 3, Madrid 28029, Spain
[7]Co-first author
*Correspondence: Alberto.Sanz@newcastle.ac.uk
http://dx.doi.org/10.1016/j.cmet.2016.03.009

SUMMARY

Increased production of reactive oxygen species (ROS) has long been considered a cause of aging. However, recent studies have implicated ROS as essential secondary messengers. Here we show that the site of ROS production significantly contributes to their apparent dual nature. We report that ROS increase with age as mitochondrial function deteriorates. However, we also demonstrate that increasing ROS production specifically through respiratory complex I reverse electron transport extends *Drosophila* lifespan. Reverse electron transport rescued pathogenesis induced by severe oxidative stress, highlighting the importance of the site of ROS production in signaling. Furthermore, preventing ubiquinone reduction, through knockdown of PINK1, shortens lifespan and accelerates aging; phenotypes that are rescued by increasing reverse electron transport. These results illustrate that the source of a ROS signal is vital in determining its effects on cellular physiology and establish that manipulation of ubiquinone redox state is a valid strategy to delay aging.

INTRODUCTION

Historically, mitochondrial ROS (mtROS) production and oxidative damage have been associated with aging and age-related diseases such as Parkinson's disease (Morais et al., 2014). In fact, the age-related increase in ROS has been viewed as a cause of the aging process (Forster et al., 1996) while mitochondrial dysfunction is considered a hallmark of aging (López-Otín et al., 2013), as a consequence of ROS accumulation. However, pioneering work in *Caenorhabidits elegans* has shown that mutations in genes encoding subunits of the electron transport chain (ETC) (Dillin et al., 2002) or genes required for biosynthesis of ubiquinone (Asencio et al., 2003; Wong et al., 1995) extend lifespan despite reducing mitochondrial function. The lifespan extension conferred by many of these alterations is ROS dependent, as reduction of ROS abolishes this effect (Lee et al., 2010; Yang and Hekimi, 2010b). Moreover, chemical inhibition of glycolysis or exposure to metabolic poisons that block respiratory complex I (CI) (rotenone, paraquat, or piericidin A) or complex III (CIII) (e.g., antimycin A) also prolong lifespan in *C. elegans* in a ROS-dependent manner (Dillin et al., 2002; Schmeisser et al., 2013; Schulz et al., 2007; Yang and Hekimi, 2010a). Various studies have shown that ROS act as secondary messengers in many cellular pathways, including those which protect against or repair damage (Ristow and Schmeisser, 2011; Yee et al., 2014). ROS-dependent activation of these protective pathways may explain their positive effect on lifespan. The confusion over the apparent dual nature of ROS may, in part, be due to a lack of resolution as without focused genetic or biochemical models it is impossible to determine the site from which ROS originate.

A promising path to resolving ROS production in vivo is the use of alternative respiratory enzymes, absent from mammals and flies, to modulate ROS generation at specific sites of the ETC (Rustin and Jacobs, 2009). The alternative oxidase (AOX) of *Ciona intestinalis* is a cyanide-resistant terminal oxidase able to reduce oxygen to water with electrons from reduced ubiquinone (CoQ), thus bypassing CIII and complex IV (CIV) (Fernandez-Ayala et al., 2009). NDI1 is a rotenone-insensitive alternative NADH dehydrogenase found in plants and fungi, which is present on the matrix-face of the mitochondrial inner membrane where it is able to oxidize NADH and reduce ubiquinone, effectively bypassing CI. Our group and others (Bahadorani et al., 2010; Sanz et al., 2010) have demonstrated that allotopic expression of NDI1 in *Drosophila melanogaster* can extend lifespan under a variety of conditions and rescue developmental lethality in flies with an RNAi-mediated decrease in CI levels.

To determine the role of increased ROS production in regulating longevity, we utilized allotopic expression of NDI1 and AOX, along with *Drosophila* genetic tools to regulate ROS production from specific sites in the ETC. We show that NDI1 over-reduces the CoQ pool and increases ROS via reverse electron transport (RET) through CI. Importantly, restoration of CoQ redox state via NDI1 expression rescued mitochondrial function and longevity in two distinct models of mitochondrial dysfunction.

This is an open access article under the CC BY-NC-ND license (http://creativecommons.org/licenses/by-nc-nd/4.0/).

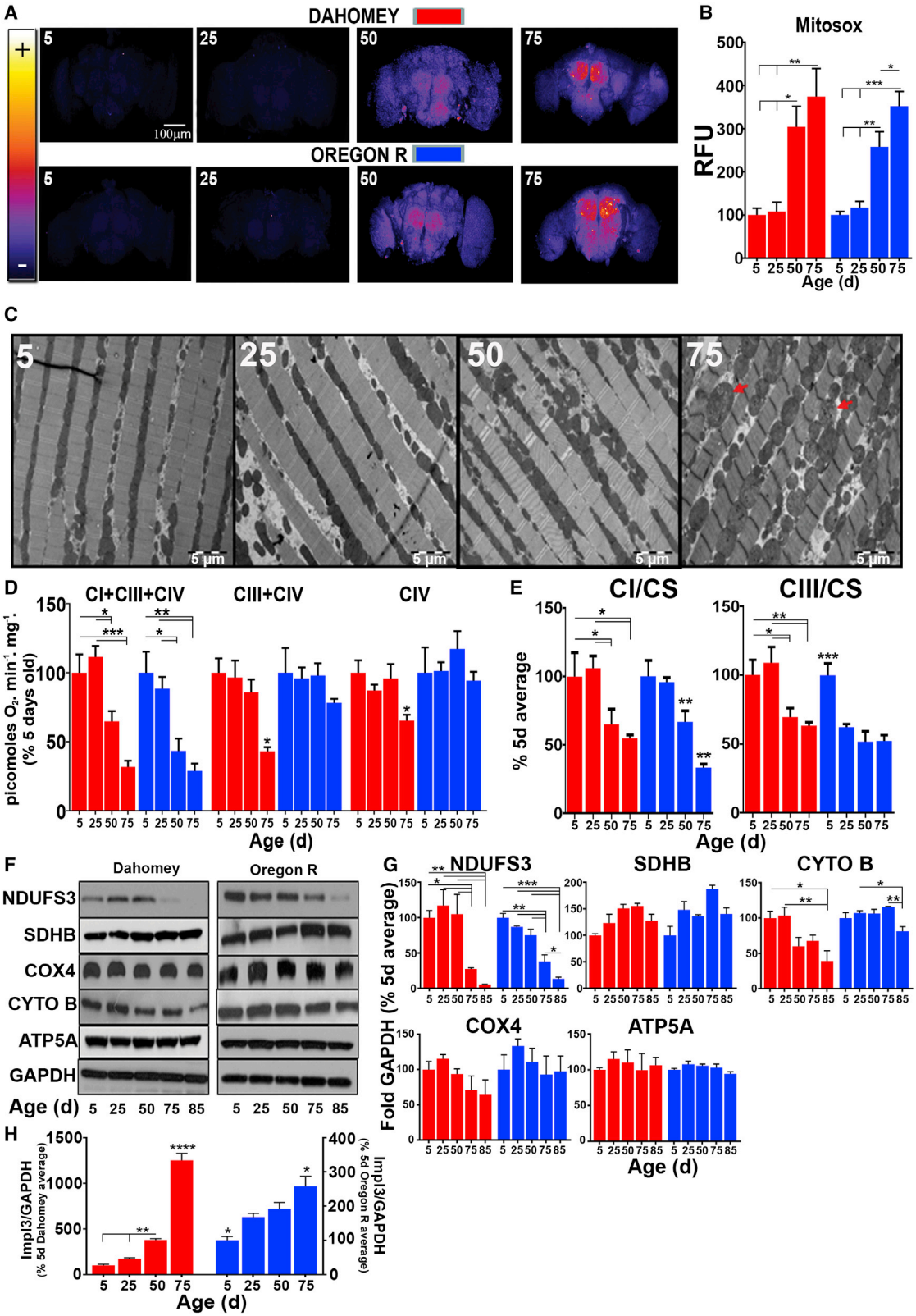

Figure 1. Increased ROS Production in Aging Flies Correlates with Mitochondrial Dysfunction

(A) Representative images of dissected fly brains stained with MitoSOX from wild-type flies of the indicated ages.

(B) Quantification of (A) (n = 5).

(legend continued on next page)

RESULTS AND DISCUSSION

ROS Production Increases with Age and Correlates with a Decrease in CI-Linked Respiration

Initially, we asked whether increased mtROS production is a general feature of aging in flies by measuring ROS production in fly brains using two fluorescent probes, MitoSOX (for mitochondrial matrix ROS) and H_2DCF (for total cellular ROS levels), and a redox-sensitive GFP based reporter for in vivo mitochondrial H_2O_2 (mtH_2O_2) (mtORP1-roGFP) (Albrecht et al., 2011). We observed a consistent increase in ROS in old flies in two wild-type strains (Dahomey and Oregon R) (Figures 1A, 1B, S1A, and S1B). In Dahomey flies, we observed that with age, dorsal flight muscle mitochondrial ultrastructure became increasingly rounded and swollen with the appearance of perturbed cristae structure at 75 days (d) (Figures 1C, S1C, and S1D). Further, in both strains, high-resolution respirometry and enzymatic assays showed a decrease in CI-linked respiration (CI-respiration from here on) and in the enzymatic activity of CI and CIII (Figures 1D and 1E). Aconitase activity initially decreased from 5 to 25 d but remained constant as the flies continued to age (Figure S1E). At this age (25 d), no decrease in locomotive activity (Figure S1F) or increase in ROS (Figures 1A, 1B, S1A, and S1B) was observed. Western blot analysis showed that only the levels of CI and aconitase were significantly affected with age (Figures 1F, 1G, and S1G–S1J). However, CI concentration was decreased at very late (75 and 85 d) ages, suggesting a shift in mitochondrial metabolism supported by an increase in *ImpL3* (*lactate dehydrogenase A homologue*) expression (Figure 1H).

Over-Reduction of the CoQ Pool Increases ROS Production and Extends Lifespan

Based on our previous results, we hypothesized that decreasing ROS and compensating for a loss in CI respiration would extend lifespan. We and others have previously reported that allotopic expression of NDI1 decreases ROS in mitochondria isolated from old individuals (Sanz et al., 2010). Surprisingly, measurement of ROS levels using MitoSOX, H_2DCF, and mtORP1-roGPF revealed in fly brains a NDI1-mediated increase in ROS that was partially abolished by AOX expression (Figures 2A, 2B, and S2B). Neither NDI1 nor AOX had any detectable effect on respiration alone (Figure S2C). Strikingly, the increase in ROS elicited by NDI1 was similar to that caused by feeding flies with a dose of rotenone able to significantly inhibit CI (Figures S2D–S2F). AOX expression completely abolished lifespan extension conferred by NDI1 (Figure 2C), suggesting that NDI1 lifespan extension is dependent on over-reduction of the ETC and consequently increased ROS levels. Expression of AOX alone had a mild effect on wild-type ROS production (Figures 2A, 2B, and S2B) and did not shorten lifespan (Figure 2C).

Based on previous studies (Owusu-Ansah et al., 2013; Yang and Hekimi, 2010a), we hypothesized that the observed NDI1-mediated increase in ROS production was perhaps a signal that led to an extension in lifespan. To further test this possibility, we generated another model in which we expressed NDI1 but alleviated the over-reduction of the ETC and prevented additional ROS formation by decreasing CI levels (via knockdown of ND-39 (*CG6020*), the fly homolog of NDUFA9, Figures 2D and S2G). These flies, hereafter referred to as CI > 2;NDI1 > daGAL4 flies, had reduced CI activity (Figure S2H) and, like AOX > 2;NDI1 > daGAL4 flies, had decreased ROS levels compared to NDI1 expressing flies (Figures 2E, 2F, and S2I). As with AOX expression, CI knockdown suppressed lifespan extension conferred by NDI1 (Figure 2G), further supporting the hypothesis that over-reduction of the ETC downstream of CI can increase ROS production and extend lifespan. To verify a change in the redox state of CoQ, we measured the percentage of reduced and oxidized CoQ in NDI1-expressing and controls flies, observing a remarkable increase in the proportion of reduced CoQ in NDI1 flies (Figure S2J). As expected, co-expression of NDI1 with AOX or decreasing CI levels restored the redox state of CoQ to normal (Figure S2J).

To exclude the possibility that the ROS signal originated downstream of CoQ, we knocked down the CIV subunit, levy (*CG17280*, fly homolog for human COX6A), to over-reduce cytochrome c and CIII in AOX-expressing flies (hereafter referred to as CIV > 2;AOX > daGAL4 flies). AOX was required in this model to maintain the CoQ pool oxidized (Figure S2K) and prevent RET through CI. CIV > 2;AOX > daGAL4 flies displayed significantly decreased CIV-linked respiration (Figure S2L) but normal food intake and body weight (Figures S2M and S2N). However, stabilization of reduced cytochrome c did not produce a ROS signal (Figure S2O) or extend lifespan (Figure S2P), supporting a site specificity for this longevity-extending ROS signal. Finally, to confirm that ROS and not changes in the redox state of CoQ were responsible for NDI1 lifespan extension, we co-expressed NDI1 with a mitochondrially targeted catalase (mtCAT) (Mockett et al., 2003) (Figure 2D; hereafter mtCAT > 2;NDI1 > daGAL4 flies). Expression of mtCAT restored H_2O_2 levels to normal (Figures 2H and 2I) without, as expected, affecting superoxide (Figure 2J) or the redox state of CoQ (Figure S2R). Since lifespan of mtCAT > 2;NDI1 > daGAL4 flies was similar to control flies, we can conclude that mtROS are responsible for NDI1 lifespan extension (Figure 2K). Significantly, expression of mtCAT alone reduced both mtH_2O_2 levels (e.g., more than AOX) and lifespan (Figure 2K), indicating that excessive reduction of ROS can be detrimental for lifespan.

To investigate how NDI1 increases ROS, we dissected mtROS production in vivo by adding specific ETC inhibitors to the food of NDI1 flies (Figure 2L). Rotenone is a specific CI Q-site inhibitor

(C) Representative EM images of Dahomey flight muscle sections at 1,000x magnification dissected at the indicated ages (n = 10, 1 muscle per fly; red arrows indicated exemplar swollen, rounded mitochondria, see Figure S1C for quantification).
(D) Mitochondrial respiration in Dahomey and Oregon R flies at the indicated ages (n = 6).
(E) CI and CIII enzymatic activity in wild-type flies of the indicated ages (n = 5).
(F) CI (NDUFS3), CII (SDHB), CIII (CYTOB), CIV (COX4), and CV (ATP5A) levels in wild-type flies. GAPDH is used as a loading control.
(G) Quantification of (F).
(H) *ImpL3* expression in wild-type flies of the indicated ages.
Values shown represent means ± SEM of at least three biological replicates, unless otherwise stated. See also Figure S1.

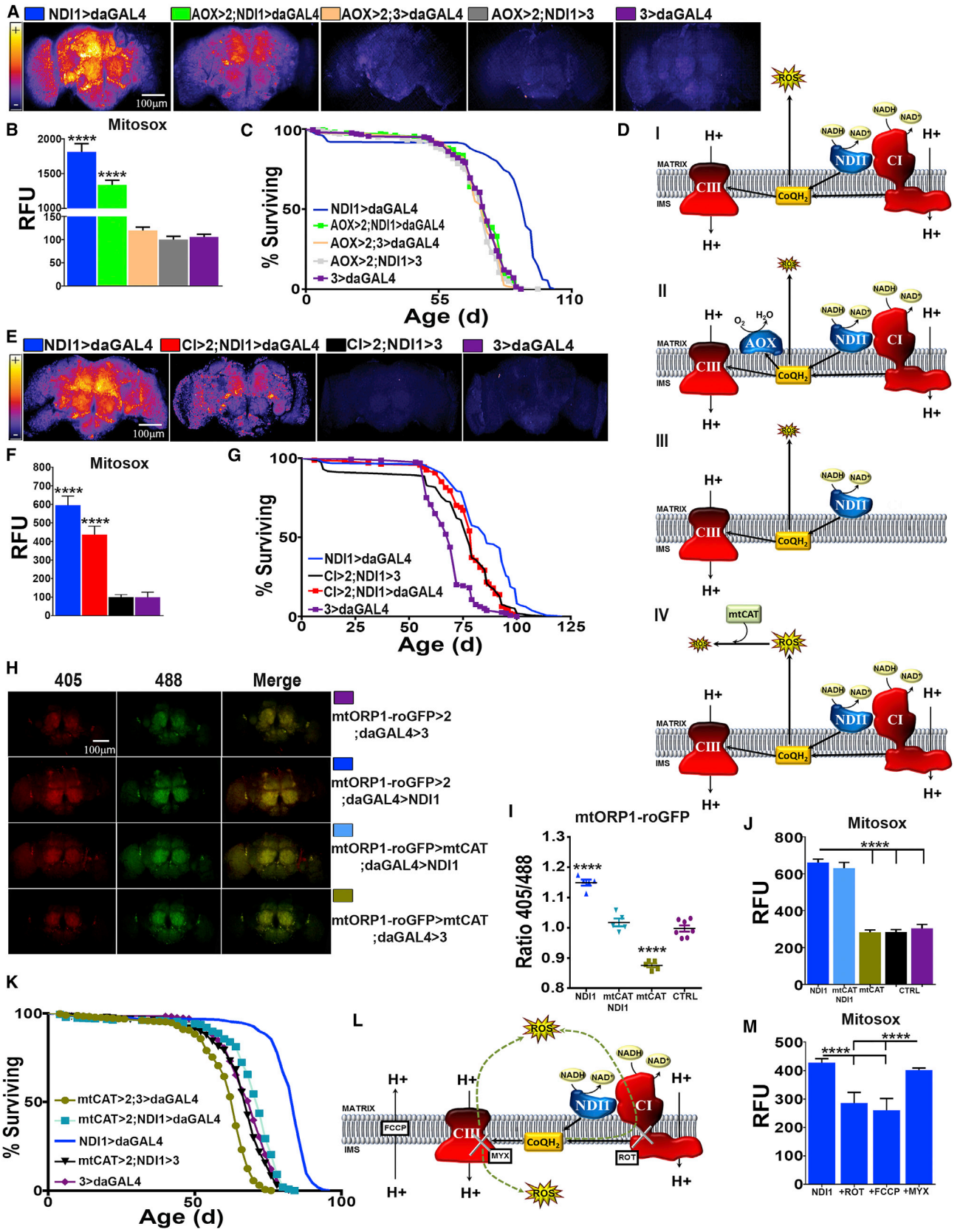

(legend on next page)

that prevents CI binding to CoQ. Rotenone feeding in wild-type flies caused a significant decrease in CI NADH:decylubiquinone (NADH:DQ) activity, while non-physiological NADH:hexaammineruthenium (NADH:HAR) activity, which is not dependent on CoQ binding, was unaffected (Figure S2F), indicating that levels of CI were not reduced. Rotenone feeding significantly decreased ROS production in NDI1 expressing flies (Figures 2M and S2T), while increasing it in wild-type flies (Figures S2D and S2E), suggesting that RET is the source of NDI1-mediated ROS production. RET in vitro is strongly membrane potential-dependent requiring a high enough membrane potential so as to make forward electron transport through CI unfavorable. Collapsing membrane potential by feeding FCCP (a H^+ ionophore) like rotenone depleted NDI1-mediated ROS production, whereas myxothiazol (a CIII Q_o site inhibitor that blocks entry of electrons into CIII) did not (Figure 2M), strongly supporting the existence of RET in vivo in NDI1-expressing flies. Interestingly, we have recently shown that during ischemia reperfusion RET is the main source of superoxide in vivo (Chouchani et al., 2014).

CoQ-Mediated ROS Signaling Can Rescue Pathology Induced by Oxidative Stress

If ROS signaling is site specific and works to maintain mitochondrial function, we hypothesized that it should be possible for beneficial ROS signaling to rescue deleterious mitochondrial phenotypes induced by oxidative stress. To test this, we knocked down SOD2 (the only mitochondrial matrix superoxide dismutase in *Drosophila*; Figure S3A) and observed a significant increase in levels of superoxide in fly brains (Figures 3A and 3B) while levels of mtH_2O_2 were significantly decreased (Figure S3B, right), which is in agreement with the reported positive correlation between SOD2 activity and mtH_2O_2 levels (Rodríguez et al., 2000). SOD2 knockdown dramatically shortened longevity (Figure 3C) and, in addition, severely affected CI-respiration (Figure 3D), with a significant decrease in the enzymatic activity of CI, CII, and aconitase (Figure 3E). Western blot analysis showed that levels of CI and aconitase were unchanged (Figure S3D), suggesting that, as has been shown for aconitase, high levels of superoxide inhibit the activity of these enzymes (Gardner and Fridovich, 1992). Mitochondrial ultrastructure from dissected dorsal flight muscle was unaffected by SOD2 knockdown (Figures S3E and S3F), showing that high levels of superoxide recapitulate some (e.g., increased mortality and, decreased CI activity), but not all features of aging (e.g., alteration in mitochondrial morphology). Although high levels of superoxide in the absence of SOD2 are detrimental, this situation is unlikely to occur in vivo in aged flies since SOD2 levels (Figures S1G and S1H) and superoxide dismutase activity (Sohal et al., 1990) are reported to increase with age.

To assess the role of CoQ-mediated ROS production, we expressed either AOX or NDI1, which have opposite effects on mtROS and the redox state of the CoQ pool, in SOD2 knockdown flies. AOX expression rescued the increase in superoxide elicited by SOD2 knockdown, but further decreased the concentration of mtH_2O_2 (Figures 3A, 3B, and S3B), and did not extend lifespan or rescue decreased ETC function (Figures 3C–3E). NDI1 expression partially rescued lifespan (Figure 3C), along with CI respiration and activity (Figures 3D and 3E), despite further increasing ROS levels (Figures 3A, 3B, and S3B). To confirm that NDI1 rescue of lifespan was mediated via RET, we reduced CI levels in SOD2 knockdown flies expressing NDI1 (hereafter SOD2 > CI; NDI1 > ActGS) using the inducible *GeneSwitch* system (Nicholson et al., 2008). Strikingly, NDI1 rescue of lifespan disappeared when RET was prevented by depletion of CI levels (Figure S3G). These results indicate that SOD2 knockdown perturbs CoQ reduction due to decreased activity of CI and CII, which results in increased superoxide production. In this model, re-establishing RET-derived ROS with NDI1 rescued CI activity, suggesting that RET may be necessary for the maintenance of mitochondrial function and lifespan extension.

Loss of CoQ-Mediated ROS Signaling Accelerates Aging

In Figure 1, we demonstrated that mitochondrial quality was decreased in aged flies. Interestingly, we also found that levels of PINK1 and Parkin decreased in parallel over time (Figures 4A and 4B). Experimental manipulation of PINK1 and Parkin levels has previously been shown to alter *Drosophila* lifespan (Rana et al., 2013; Todd and Staveley, 2012). Decreases in

Figure 2. NDI1 Increases ROS Production via Over-Reduction of CoQ

(A) Representative images of dissected brains from indicated genotypes stained with MitoSOX.

(B) Quantification of (A) (n = 5).

(C) Survival curves for the indicated genotypes (n = 200).

(D) Schematic diagram illustrating effects of expressing two different alternative respiratory enzymes on electron transport: (i) NDI1 generates ROS by over-reducing the CoQ pool; (ii) AOX reverts the effects of NDI1 by re-oxidizing the CoQ pool; (iii) decrease in the levels of CI can prevent reduction of CoQ and subsequent ROS production; (iv) ectopic expression of mtCAT reduces ROS levels without altering mitochondrial respiration or the redox state of CoQ .

(E) Representative images of brains from the indicated genotypes stained with MitoSOX.

(F) Quantification of (E) (n = 5).

(G) Survival curves for the indicated genotypes (n = 160).

(H) In vivo ROS measurements from indicated genotypes in brains dissected from flies expressing a mitochondrially localized redox-sensitive GFP-based reporter.

(I) Quantification of (H) (n = 5–7).

(J) Quantification of brains dissected from flies of the indicated genotypes stained with MitoSOX (n = 5).

(K) Survival curves for the indicated genotypes (n = 200).

(L) Diagram illustrating using metabolic poisons to dissect ROS production: rotenone (ROT), carbonyl cyanide-p-trifluoromethoxyphenylhydrazone (FCCP), or myxothiazol (MYX). Green dashed arrows indicate the possible flow of electrons following CoQ reduction.

(M) Quantification of brains dissected from NDI1 flies fed with metabolic poisons, stained with MitoSOX (n = 4).

Values shown represent means ± SEM of at least 3 biological replicates, unless otherwise stated.

See also Figure S2 and Table S1 for statistical analysis of survival curves.

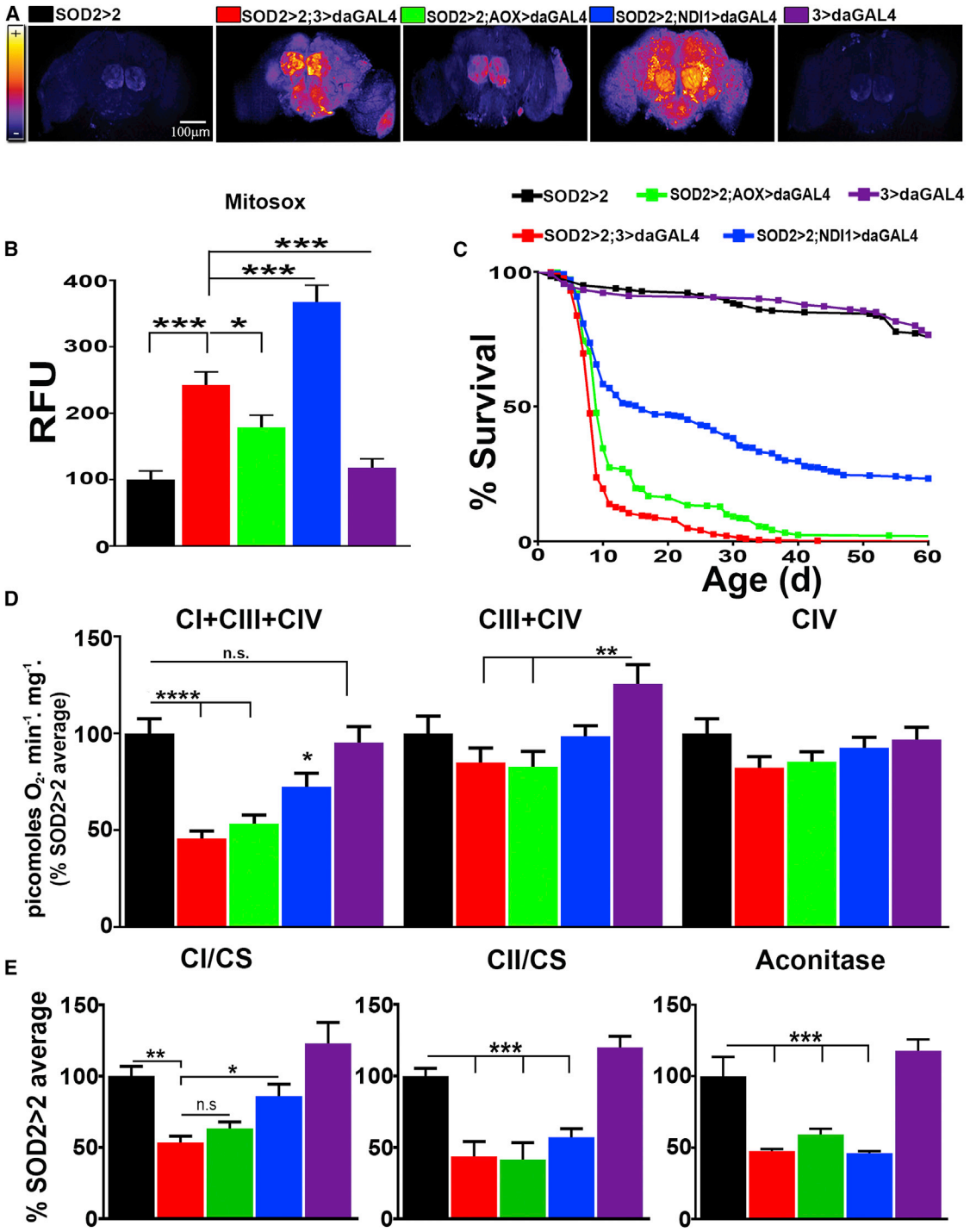

Figure 3. NDI1-Mediated ROS Production Rescues Superoxide-Mediated Mitochondrial Dysfunction

(A) Representative images of fly brains from indicated genotypes stained with MitoSOX.

(B) Quantification of (A) (n = 5).

(C) Survival curves of the indicated genotypes (n = 180–380).

(D) Mitochondrial respiration in flies of the indicated genotypes (n = 6).

(E) CI, CII, and aconitase enzymatic activities in flies of the indicated genotypes (n = 7).

Values shown represent means ± SEM of at least three biological replicates, unless otherwise stated. See also Figure S3 and Table S1 for statistical analysis of survival curves.

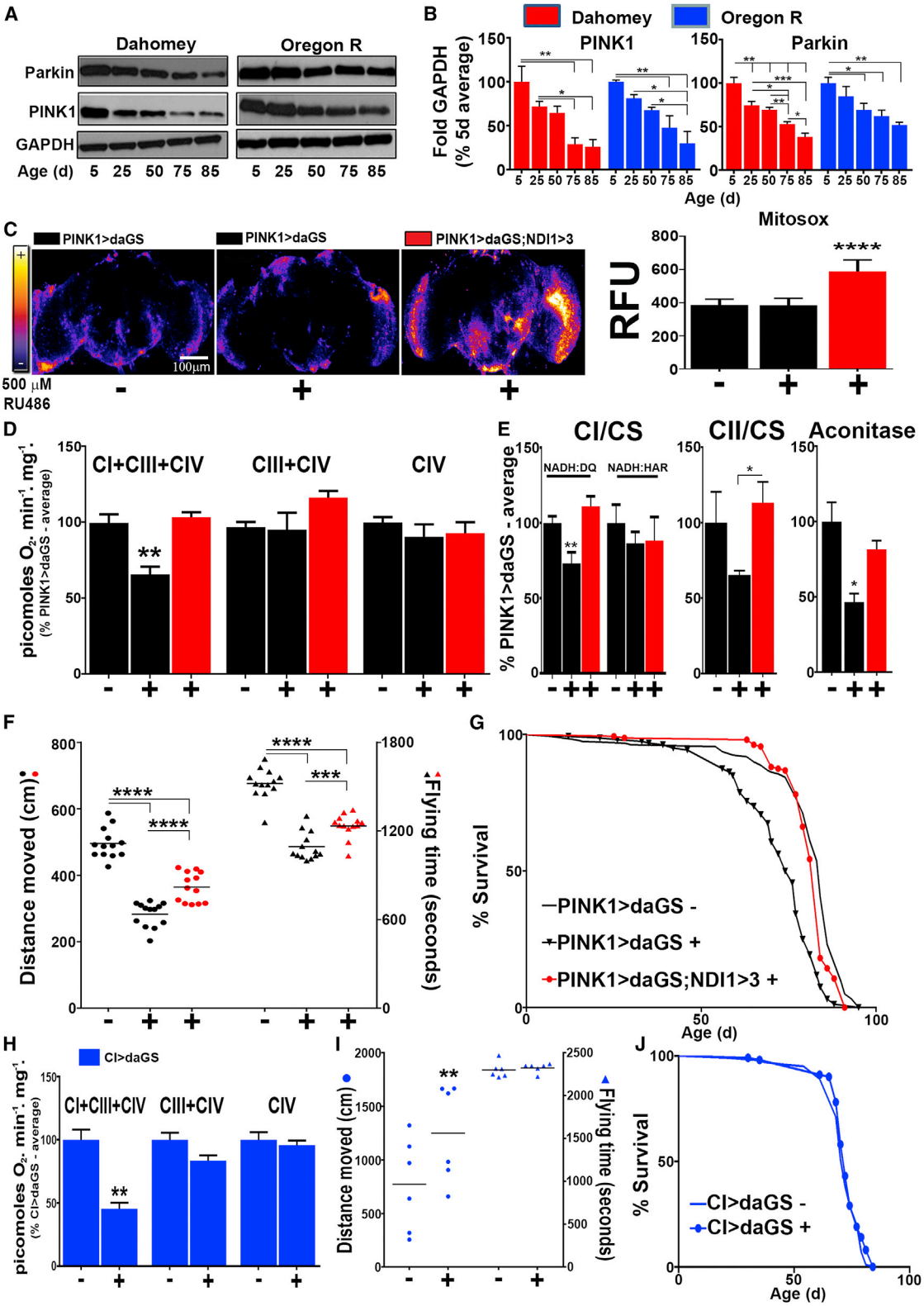

Figure 4. Re-Establishing the Redox State of CoQ Prevents Age-Related Pathology

(A) PINK1 and Parkin levels in wild-type flies during aging.

(B) Quantification of (A).

(C) Representative images and quantification of dissected fly brains stained with MitoSOX (quantification n = 7).

(legend continued on next page)

PINK1 activity have been related to a loss of CI activity (Morais et al., 2014), while *Parkin* loss of function mutations cause the accumulation of aberrant mitochondria (Greene et al., 2003). Strikingly, decreases in PINK1 and Parkin levels (Figures 4A and 4B) preceded the decline in respiration observed in old flies (Figure 1D). We hypothesized that this may contribute to the mitochondrial dysfunction that occurs with age. It has been recently shown that PINK1 is required for reduction of CoQ by CI via phosphorylation of NDUFA10 (Morais et al., 2014), although this was not confirmed by a later report (Pogson et al., 2014). Since PINK1 protein levels decrease with age, we hypothesized that this decrease could be responsible for the decline in CI-respiration. To test the relevance of CoQ-mediated ROS signaling in a more physiological context, we used the inducible GeneSwitch system to drive expression of an RNAi construct against PINK1 specifically in adult flies (PINK1 > daGS flies, Figure S4A). PINK1 knockdown did not increase ROS levels (Figures 4C and S4B); however, we did observe a significant decrease in CI-linked respiration (Figure 4D) and NADH:DQ CI activity, but not NADH:HAR activity (Figure 4E) or CI protein levels (Figure S4C), showing that reduction of CoQ by CI was impaired, as was observed in SOD2 knockdown flies (Figures 3D and 3E) and 50-d-old wild-type flies (Figures 1D and 1E). Furthermore, PINK1 knockdown flies displayed decreased mobility, time spent flying, and lifespan compared to controls (Figures 4F and 4G).

As in SOD2 knockdown flies, NDI1-mediated ROS production (Figure 4C) was able to rescue CI-linked respiration and CI activity in PINK1 knockdown flies (Figures 4D and 4E). However, unlike in SOD2 knockdown flies, CII and aconitase activities were also rescued (Figure 4E), suggesting that SOD2 may be necessary for NDI1-mediated rescue of CII and aconitase. Locomotive activity, time spent flying, and lifespan were also partially or totally rescued by NDI1 expression in PINK1 knockdown flies (Figures 4F and 4G). Interestingly, reduction of CI levels from adulthood decreased CI respiration to levels comparable with 50-d-old wild-type flies and PINK1 knockdown flies (Figure 4H), whereas locomotion and lifespan were similar to that observed in flies with induction of the driver alone (Compare Figures 4I and 4J with Figures S4D–S4G). Moreover, NDI1 did not restore respiration in this background (data not shown), just as it failed to when CI knockdown and NDI1 expression were driven with a stronger driver (Figure S2C). This indicates that the rescue of mitochondrial function conferred by NDI1 in SOD2 and PINK1 knockdown flies is not due to direct compensation by NDI1 of decreased CI activity, rather NDI1 rescues CI function through over-reduction of the CoQ pool. Therefore, we propose that over-reduction of CoQ pool generates, via RET, a ROS signal necessary for homeostasis. Interruption in electron flow through CI would prevent CoQ reduction and thus cause the deleterious phenotypes associated with aging and age-related pathologies.

In summary, we show that mtROS production increases with age and that un-detoxified ROS can be detrimental to *Drosophila* lifespan, while increasing ROS production specifically from reduced CoQ, possibly via RET, acts as a signal to maintain mitochondrial function (notably CI) and extend lifespan (Figure S4J). These results are similar to those reported in worms where small doses of rotenone (Schmeisser et al., 2013), paraquat, and mutations in CI that increase ROS extend lifespan (Yang and Hekimi, 2010a). However, we did not observe lifespan extension in flies fed with varying doses of rotenone or paraquat (Figures S4H and S4I). It is possible that an intact CI is required for lifespan extension in fruit flies, as metformin, which increases lifespan by blocking CI and increasing ROS in worms (De Haes et al., 2014), fails to do so in fruit flies (Slack et al., 2012). If the mechanism we describe here is conserved in mammals, manipulation of the redox state of CoQ may be a strategy for the extension of both mean and maximum lifespan and the road to new therapeutic interventions for aging and age-related diseases.

EXPERIMENTAL PROCEDURES

Fly Husbandry

Female flies were used in all experiments. See Table S2 for details of the different fly strains used in this study. Flies were maintained at 25°C on standard media in a controlled 12:12 hr light:dark cycle at a density of 20 flies/vial and transferred to new food every 2 to 3 d. For all lifespan experiments, at least 80 flies were used and each experiment was repeated at least two to four times. Statistical analysis for all lifespan experiments can be found in Table S1.

ROS Detection

MitoSOX and dichlorofluorescein (H_2DCF) were used to measure either mitochondrial matrix superoxide or total cellular ROS levels, respectively. Following dissection, fly brains were incubated in MitoSOX or H_2DCF for 10 min and imaged immediately. For in vivo ROS imaging brains dissected from lines carrying the mtORP1-roGFP reporter construct were imaged under Ex. 488 (reduced) or 405 (oxidized) nm/Em. 510 nm. The total (average) fluorescence intensity of each individual brain imaged was quantified using ImageJ.

Electron Microscopy

Dorsal flight muscles were dissected and suspended in 0.16 M sym-collidine buffer pH 7.4 (Electron Microscopy Sciences) supplemented with 5% glutaraldehyde (fixing solution). Muscle sections were imaged using a JEOL JEM-1400 Plus transmission electron microscope fitted with an 11 Mpx Olympus Quemesa digital camera. The images were manually segmented using GIMP (http://www.gimp.org/), and the resulting segmented image was further analyzed using the ImageJ particle analysis tool.

High-Resolution Respirometry

Respirometry measurements of whole-fly homogenates were performed using an OROBOROS O2k oxygraph. State 4 respiration was initiated by addition of

(D) Mitochondrial respiration in flies of the indicated genotypes.
(E) CI, CII, and aconitase activities in flies of the indicated genotypes (n = 4–8).
(F) Locomotive activity and flying time in flies of the indicated genotypes (n = 13).
(G) Survival curves for the indicated genotypes (n = 160).
(H) Mitochondrial respiration in flies of the indicated genotypes (n = 5).
(I) Locomotive activity and flying time in flies of the indicated genotypes (n = 6).
(J) Survival curves for the indicated genotypes (n = 160).
Values shown represent means ± SEM of at least three biological replicates, unless otherwise stated. −/+ indicates absence/presence of 500 μM RU-486 during adulthood. See also Figure S4 and Table S1 for statistical analysis of survival curves.

5 mM pyruvate and 5 mM proline. State 3 was initiated with the addition of 1 mM ADP. CI-linked respiration (CI+CIII+CIV in figures) was inhibited by adding 0.5 μM rotenone, and CIII-linked respiration was stimulated by addition of 20 mM glycerol 3-phosphate (CIII+CIV in figures). CIII-linked respiration was inhibited with the addition of 2.5 μM antimycin A. CIV respiration (CIV in figures) was initiated by the addition of 4 mM ascorbate and 2 mM TMPD. CIV respiration was inhibited by adding 0.5 mM KCN. Data presented correspond to state 3 respiration (i.e., after ADP addition).

Enzymatic Assays

All assays were adapted to a 96-well plate with a final volume of 300 μl. CI (NADH dehydrogenase or NADH: hexaammineruthenium (HAR) oxidoreductase activity), CII (malonate-sensitive succinate:dichlorophenolindophenol (DCPIP) oxidoreductase activity), CIII (antimycin-sensitive decylubiquinol: cytochrome c oxidoreductase activity), CIV (potassium cyanide-sensitive cytochrome c oxidase activity), CV (oligomycin-sensitive NADH-coupled ATPase activity), and mitochondrial aconitase activities were measured according to standard procedures. All ETC activities were normalized to mitochondrial density calculated by citrate synthase (CS).

Behavioral and Locomotive Activity Assays

Live tracking of the flies was performed using a high-sensitivity The Imaging Source USB camera (equipped with a Computar 1/3" Varifocal Lens [2.8–12 mm]), for 60 min per experiment. The recorded video files were used to calculate distance moved per hour for each fly using the EthoVision XT video tracking software (Noldus Information Technology).

Statistical Analysis

Values shown represent means ± SEM. Data were analyzed with Prism 6 (GraphPad) using either one-way ANOVA with Newman-Keul's post hoc test or using the unpaired Student's t test. Lifespan data were analyzed using the log-rank Mantel Cox Test. $p < 0.05$ was taken as statistically significant. In all figures $^{*}p < 0.05$, $^{**}p < 0.01$, $^{***}p < 0.005$, and $^{****}p < 0.001$ denotes significant difference from all other groups unless otherwise indicated by line art. NS, not significantly different. Individual and pooled lifespan experiments with statistical analysis are summarized in Table S1.

SUPPLEMENTAL INFORMATION

Supplemental Information includes four figures, two tables, and Supplemental Experimental Procedures and can be found with this article online at http://dx.doi.org/10.1016/j.cmet.2016.03.009.

AUTHOR CONTRIBUTIONS

F.S., A. Sriram, D.F.-A., N.G., M.L., G.N., A.L., H.M.C., and P.N. performed experiments and analyzed data. M.P.M. and J.A.E. designed research and co-wrote the manuscript. A. Sanz designed and performed experiments, supervised the project, and co-wrote the manuscript.

ACKNOWLEDGMENTS

This work was supported by the European Research Council (ERC Starting Grant to A. Sanz), the Academy of Finland (Academy Research Fellowship to A. Sanz and Postdoctoral Research grant to H.M.C), the BBSRC (Responsive mode grant to A. Sanz), the Centre for International Mobility (Postdoctoral fellowship to N.G.), the Medical Research Council (M.P.M), and the Spanish Ministry of Health and the Instituto de Salud Carlos III (FIS PI14-01962 to P.N.). Electron microscopy image processing was performed at the Laboratory of Electron Microscopy, University of Turku, Finland. We thank Dr Rhoda Stefanatos for help with editing the manuscript. The authors declare no competing financial interests.

Received: January 16, 2015
Revised: January 26, 2016
Accepted: March 24, 2016
Published: April 12, 2016

REFERENCES

Albrecht, S.C., Barata, A.G., Grosshans, J., Teleman, A.A., and Dick, T.P. (2011). In vivo mapping of hydrogen peroxide and oxidized glutathione reveals chemical and regional specificity of redox homeostasis. Cell Metab. *14*, 819–829.

Asencio, C., Rodríguez-Aguilera, J.C., Ruiz-Ferrer, M., Vela, J., and Navas, P. (2003). Silencing of ubiquinone biosynthesis genes extends life span in Caenorhabditis elegans. FASEB J. *17*, 1135–1137.

Bahadorani, S., Cho, J., Lo, T., Contreras, H., Lawal, H.O., Krantz, D.E., Bradley, T.J., and Walker, D.W. (2010). Neuronal expression of a single-subunit yeast NADH-ubiquinone oxidoreductase (Ndi1) extends Drosophila lifespan. Aging Cell *9*, 191–202.

Chouchani, E.T., Pell, V.R., Gaude, E., Aksentijević, D., Sundier, S.Y., Robb, E.L., Logan, A., Nadtochiy, S.M., Ord, E.N., Smith, A.C., et al. (2014). Ischaemic accumulation of succinate controls reperfusion injury through mitochondrial ROS. Nature *515*, 431–435.

De Haes, W., Frooninckx, L., Van Assche, R., Smolders, A., Depuydt, G., Billen, J., Braeckman, B.P., Schoofs, L., and Temmerman, L. (2014). Metformin promotes lifespan through mitohormesis via the peroxiredoxin PRDX-2. Proc. Natl. Acad. Sci. USA *111*, E2501–E2509.

Dillin, A., Hsu, A.L., Arantes-Oliveira, N., Lehrer-Graiwer, J., Hsin, H., Fraser, A.G., Kamath, R.S., Ahringer, J., and Kenyon, C. (2002). Rates of behavior and aging specified by mitochondrial function during development. Science *298*, 2398–2401.

Fernandez-Ayala, D.J., Sanz, A., Vartiainen, S., Kemppainen, K.K., Babusiak, M., Mustalahti, E., Costa, R., Tuomela, T., Zeviani, M., Chung, J., et al. (2009). Expression of the Ciona intestinalis alternative oxidase (AOX) in Drosophila complements defects in mitochondrial oxidative phosphorylation. Cell Metab. *9*, 449–460.

Forster, M.J., Dubey, A., Dawson, K.M., Stutts, W.A., Lal, H., and Sohal, R.S. (1996). Age-related losses of cognitive function and motor skills in mice are associated with oxidative protein damage in the brain. Proc. Natl. Acad. Sci. USA *93*, 4765–4769.

Gardner, P.R., and Fridovich, I. (1992). Inactivation-reactivation of aconitase in Escherichia coli. A sensitive measure of superoxide radical. J. Biol. Chem. *267*, 8757–8763.

Greene, J.C., Whitworth, A.J., Kuo, I., Andrews, L.A., Feany, M.B., and Pallanck, L.J. (2003). Mitochondrial pathology and apoptotic muscle degeneration in Drosophila parkin mutants. Proc. Natl. Acad. Sci. USA *100*, 4078–4083.

Lee, S.J., Hwang, A.B., and Kenyon, C. (2010). Inhibition of respiration extends C. elegans life span via reactive oxygen species that increase HIF-1 activity. Curr. Biol. *20*, 2131–2136.

López-Otín, C., Blasco, M.A., Partridge, L., Serrano, M., and Kroemer, G. (2013). The hallmarks of aging. Cell *153*, 1194–1217.

Mockett, R.J., Bayne, A.C., Kwong, L.K., Orr, W.C., and Sohal, R.S. (2003). Ectopic expression of catalase in Drosophila mitochondria increases stress resistance but not longevity. Free Radic. Biol. Med. *34*, 207–217.

Morais, V.A., Haddad, D., Craessaerts, K., De Bock, P.J., Swerts, J., Vilain, S., Aerts, L., Overbergh, L., Grünewald, A., Seibler, P., et al. (2014). PINK1 loss-of-function mutations affect mitochondrial complex I activity via NdufA10 ubiquinone uncoupling. Science *344*, 203–207.

Nicholson, L., Singh, G.K., Osterwalder, T., Roman, G.W., Davis, R.L., and Keshishian, H. (2008). Spatial and temporal control of gene expression in Drosophila using the inducible GeneSwitch GAL4 system. I. Screen for larval nervous system drivers. Genetics *178*, 215–234.

Owusu-Ansah, E., Song, W., and Perrimon, N. (2013). Muscle mitohormesis promotes longevity via systemic repression of insulin signaling. Cell *155*, 699–712.

Pogson, J.H., Ivatt, R.M., Sanchez-Martinez, A., Tufi, R., Wilson, E., Mortiboys, H., and Whitworth, A.J. (2014). The complex I subunit NDUFA10 selectively rescues Drosophila pink1 mutants through a mechanism independent of mitophagy. PLoS Genet. *10*, e1004815.

Rana, A., Rera, M., and Walker, D.W. (2013). Parkin overexpression during aging reduces proteotoxicity, alters mitochondrial dynamics, and extends lifespan. Proc. Natl. Acad. Sci. USA *110*, 8638–8643.

Ristow, M., and Schmeisser, S. (2011). Extending life span by increasing oxidative stress. Free Radic. Biol. Med. *51*, 327–336.

Rodríguez, A.M., Carrico, P.M., Mazurkiewicz, J.E., and Meléndez, J.A. (2000). Mitochondrial or cytosolic catalase reverses the MnSOD-dependent inhibition of proliferation by enhancing respiratory chain activity, net ATP production, and decreasing the steady state levels of H(2)O(2). Free Radic. Biol. Med. *29*, 801–813.

Rustin, P., and Jacobs, H.T. (2009). Respiratory chain alternative enzymes as tools to better understand and counteract respiratory chain deficiencies in human cells and animals. Physiol. Plant. *137*, 362–370.

Sanz, A., Soikkeli, M., Portero-Otín, M., Wilson, A., Kemppainen, E., McIlroy, G., Ellilä, S., Kemppainen, K.K., Tuomela, T., Lakanmaa, M., et al. (2010). Expression of the yeast NADH dehydrogenase Ndi1 in Drosophila confers increased lifespan independently of dietary restriction. Proc. Natl. Acad. Sci. USA *107*, 9105–9110.

Schmeisser, S., Priebe, S., Groth, M., Monajembashi, S., Hemmerich, P., Guthke, R., Platzer, M., and Ristow, M. (2013). Neuronal ROS signaling rather than AMPK/sirtuin-mediated energy sensing links dietary restriction to lifespan extension. Mol. Metab. *2*, 92–102.

Schulz, T.J., Zarse, K., Voigt, A., Urban, N., Birringer, M., and Ristow, M. (2007). Glucose restriction extends Caenorhabditis elegans life span by inducing mitochondrial respiration and increasing oxidative stress. Cell Metab. *6*, 280–293.

Slack, C., Foley, A., and Partridge, L. (2012). Activation of AMPK by the putative dietary restriction mimetic metformin is insufficient to extend lifespan in Drosophila. PLoS ONE *7*, e47699.

Sohal, R.S., Arnold, L., and Orr, W.C. (1990). Effect of age on superoxide dismutase, catalase, glutathione reductase, inorganic peroxides, TBA-reactive material, GSH/GSSG, NADPH/NADP+ and NADH/NAD+ in Drosophila melanogaster. Mech. Ageing Dev. *56*, 223–235.

Todd, A.M., and Staveley, B.E. (2012). Expression of Pink1 with α-synuclein in the dopaminergic neurons of Drosophila leads to increases in both lifespan and healthspan. Genet. Mol. Res. *11*, 1497–1502.

Wong, A., Boutis, P., and Hekimi, S. (1995). Mutations in the clk-1 gene of Caenorhabditis elegans affect developmental and behavioral timing. Genetics *139*, 1247–1259.

Yang, W., and Hekimi, S. (2010a). A mitochondrial superoxide signal triggers increased longevity in Caenorhabditis elegans. PLoS Biol. *8*, e1000556.

Yang, W., and Hekimi, S. (2010b). Two modes of mitochondrial dysfunction lead independently to lifespan extension in Caenorhabditis elegans. Aging Cell *9*, 433–447.

Yee, C., Yang, W., and Hekimi, S. (2014). The intrinsic apoptosis pathway mediates the pro-longevity response to mitochondrial ROS in C. elegans. Cell *157*, 897–909.

Cell Metabolism, Volume *23*

Supplemental Information

Mitochondrial ROS Produced via Reverse Electron Transport Extend Animal Lifespan

Filippo Scialò, Ashwin Sriram, Daniel Fernández-Ayala, Nina Gubina, Madis Lõhmus, Glyn Nelson, Angela Logan, Helen M. Cooper, Plácido Navas, Jose Antonio Enríquez, Michael P. Murphy, and Alberto Sanz

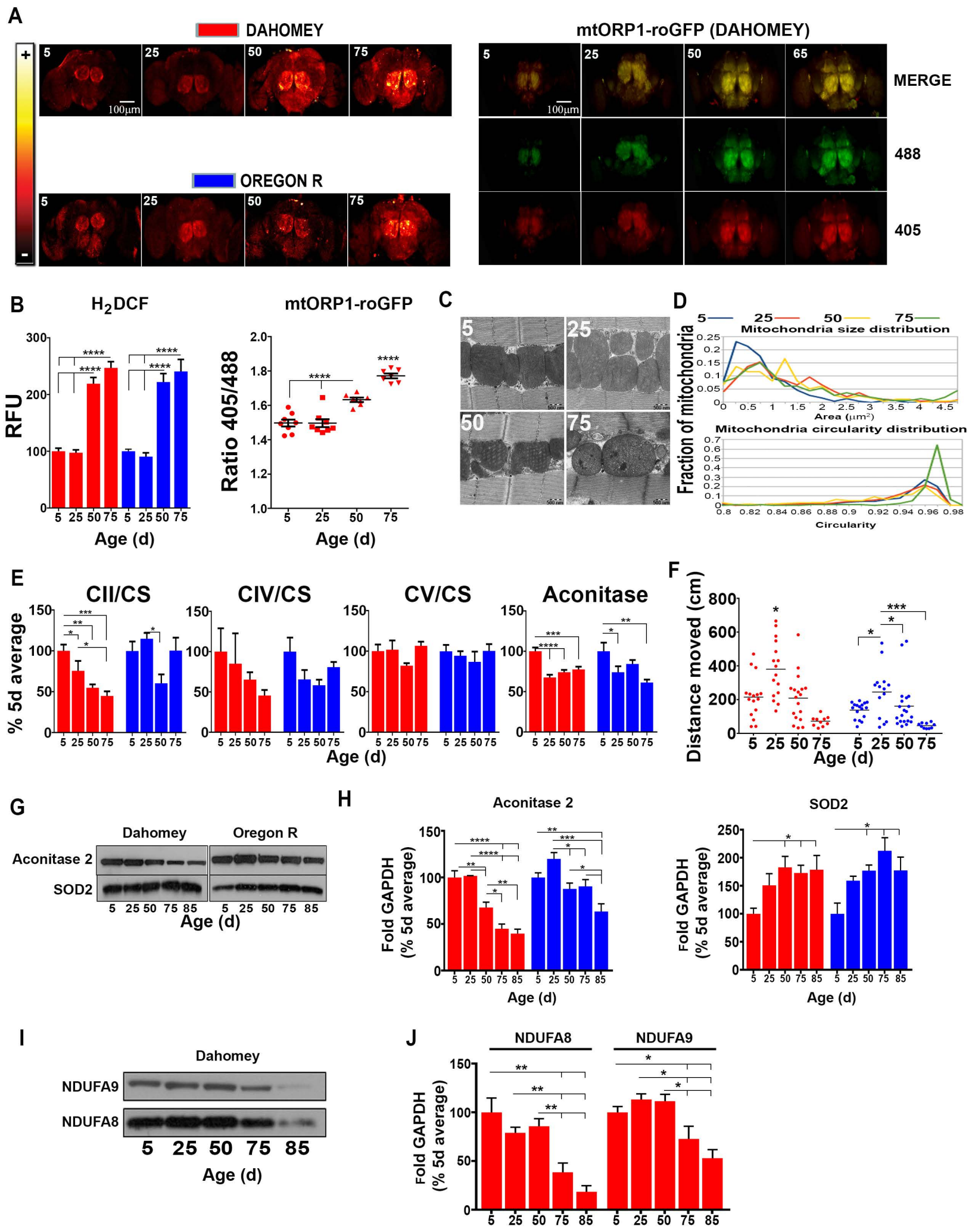

Sciaò *et al.* Supplemental Figure 1

Supplemental Figure 1. Related to Figure 1. Increased ROS production in aging flies correlates with mitochondrial dysfunction.

(A) Representative images of dissected fly brains stained with H_2DCF (left) from Dahomey and Oregon R of indicated ages and *in vivo* ROS measurements in brains dissected from Dahomey flies expressing a mitochondrially-localised redox-active GFP-based reporter (mtORP1-roGFP) of indicated ages.

(B) Quantification of A (n=7-8).

(C) Representative EM images of dissected female Dahomey dorsal flight muscle mitochondria at the indicated ages at 12000x magnification.

(D) Quantification of mitochondrial size (top) and circularity (bottom) in Figure 1C (5d, n=1069; 25d, n=753; 50d, n=901; 75d, n=744).

(E) Enzymatic activities in Dahomey and Oregon R flies (n=6).

(F) Locomotion (cms moved in 1 hour) for wild-type flies at different ages (n=10-20).

(G) Representative western blots.

(H) Quantification of **G**.

(I) Representative western blots for other CI subunits in Dahomey flies at different ages.

(J) Quantification of **I**.

Values shown represent means ± SEM of at least 3 biological replicates, unless otherwise stated.

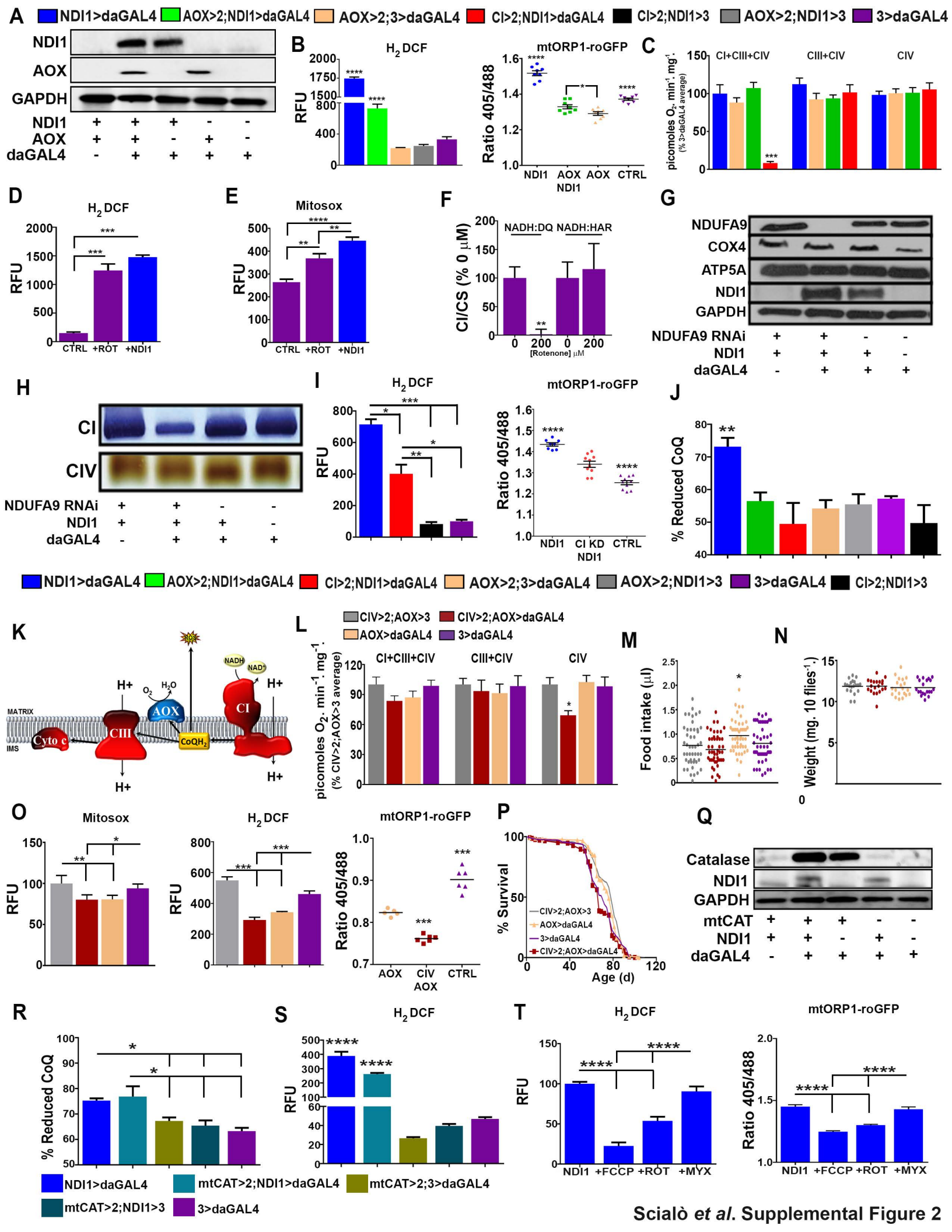

Scialò *et al.* Supplemental Figure 2

Supplemental Figure 2. Related to Figure 2. Interrogating how NDI1 produces ROS and extends lifespan.

(A) Representative western blots showing expression of NDI1 and AOX.

(B) Quantification of fly brains dissected from the indicated genotypes stained with H_2DCF (n=5) or expressing mtORP1-roGFP (n=7-8).

(C) Mitochondrial respiration from flies of the indicated genotypes (n=3-18).

(D) Quantification of fluorescence from dissected fly brains stained with H_2DCF with (NDI1>daGAL4) and without (CTRL) NDI1 or rotenone (200 µM) treatment (+ROT) (n=5).

(E) Quantification of fluorescence from dissected fly brains stained with MitoSOX with (NDI1>daGAL4) and without (CTRL) NDI1 or rotenone (200 µM) treatment (+ROT) (n=5).

(F) CI activities in rotenone-fed wild-type flies.

(G) Representative western blots for ND-39/NDUFA9 (CI subunit), COXIV (CIV subunit), ATP5A (CV subunit) and NDI1 (GAPDH serves as loading control) in the indicated genotypes.

(H) Representative activity-stained blue-native gel for CI and CIV from fly mitochondria of the indicated phenotypes.

(I) Quantification of fluorescence in dissected fly brains from CI>2;NDI1>daGAL4 flies and controls stained with H_2DCF (n=5) or expressing mtORP1-roGFP (n=8-10).

(J) Percentage of reduced CoQ in flies of the indicated genotypes.

(K) Diagram depicting the strategy (i.e. reduction of CIV levels) to specifically over-reduce ETC downstream of the CoQ pool to localize the ROS signal.

(L) Mitochondrial respiration in flies of the indicated phenotypes (n=6).

(M, N) Food intake (n=50) and body weight (n=20) in CIV>2;AOX>daGAL4 flies and controls.

(O) Quantification of brains dissected from flies of the indicated genotypes stained with MitoSOX, H_2DCF or expressing mtORP1-roGFP (n=5).

(P) Survival curves of the indicated genotypes (n=200). See Table S1 for statistical analysis.

(Q) Representative western blots showing expression of Catalase, NDI1 and AOX.

(R) Percentage of reduced CoQ in flies of the indicated genotypes (n=4-5).

(S) Quantification of brains dissected from flies of the indicated genotypes stained with H_2DCF (n=4-5).

(T) Quantification of brains dissected from NDI1>daGAL4 flies fed with the indicated metabolic poisons, stained with H_2DCF (n=5) or expressing mtORP1-roGFP (n=7-10).

Values shown represent means ± SEM of at least 3 biological replicates, unless otherwise stated.

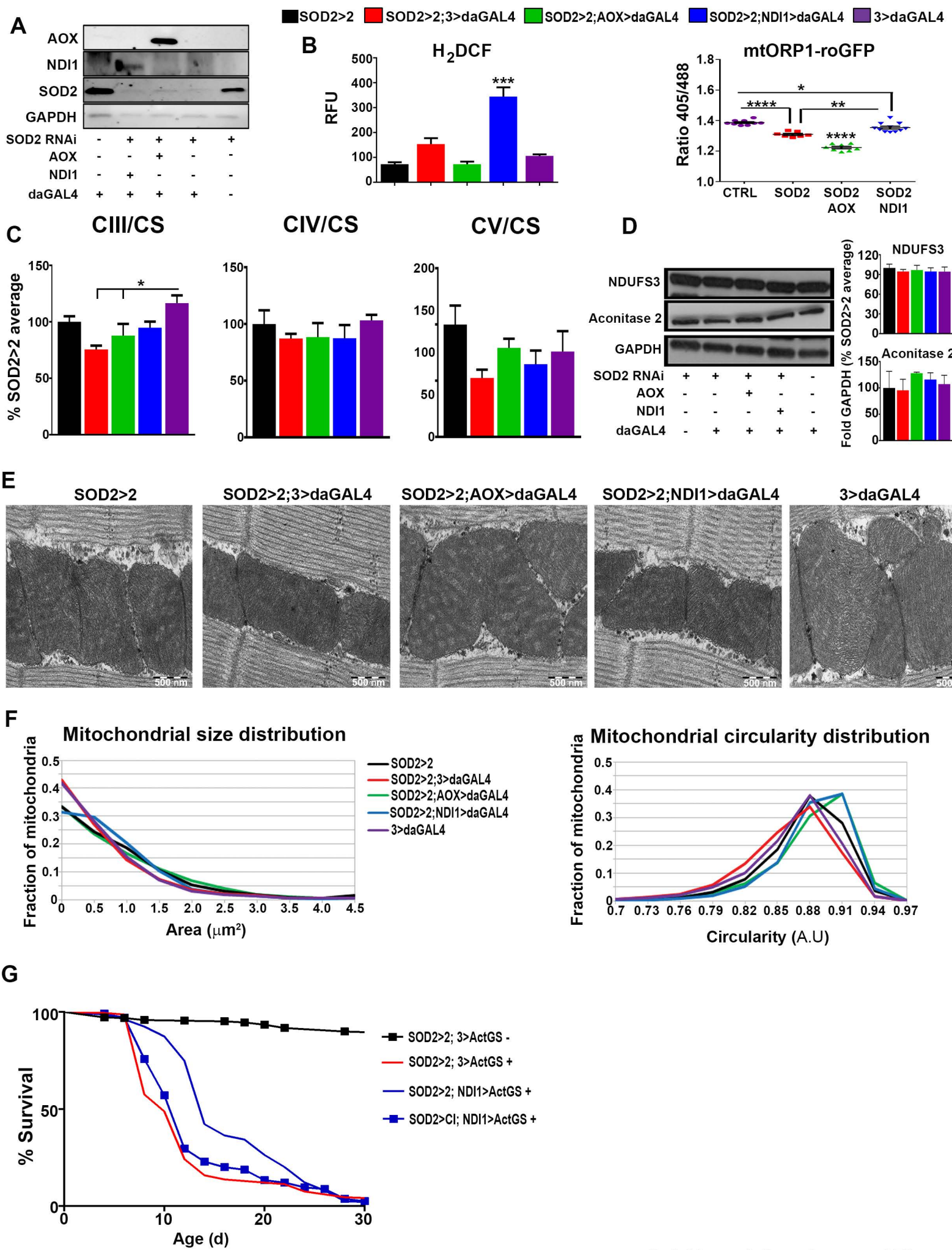

Scialò *et al.* Supplemental Figure 3

Supplemental Figure 3. Related to Figure 3. Effects of SOD2 knockdown together with co-expression of NDI1 or AOX on mitochondrial function.

(A) Representative western blot showing SOD2, AOX and NDI1 levels in the indicated genotypes.

(B) Quantification of brains dissected from flies of the indicated genotypes stained with H_2DCF (n=4) or expressing mtORP1-roGFP (n=7).

(C) Enzymatic assays showing activity of CIII, CIV (n=4) and CV in the indicated genotypes.

(D) Representative western blots and quantification of levels of NDUFS3 (CI subunit) and Aconitase 2 in the indicated genotypes (GAPDH is used as a loading control)

(E) Representative electron micrographs of dissected dorsal flight muscle mitochondria (20,000x magnification) from the indicated genotypes.

(F) Quantification of mitochondrial size (left) and circularity (right) in **E**.

(G) Survival curves of indicated genotypes (n=120-180). -/+ indicates presence/absence of 300 µM RU-486. See Table S1 for statistical analysis.

Values shown represent means ± SEM of at least 3 biological replicates, unless otherwise stated.

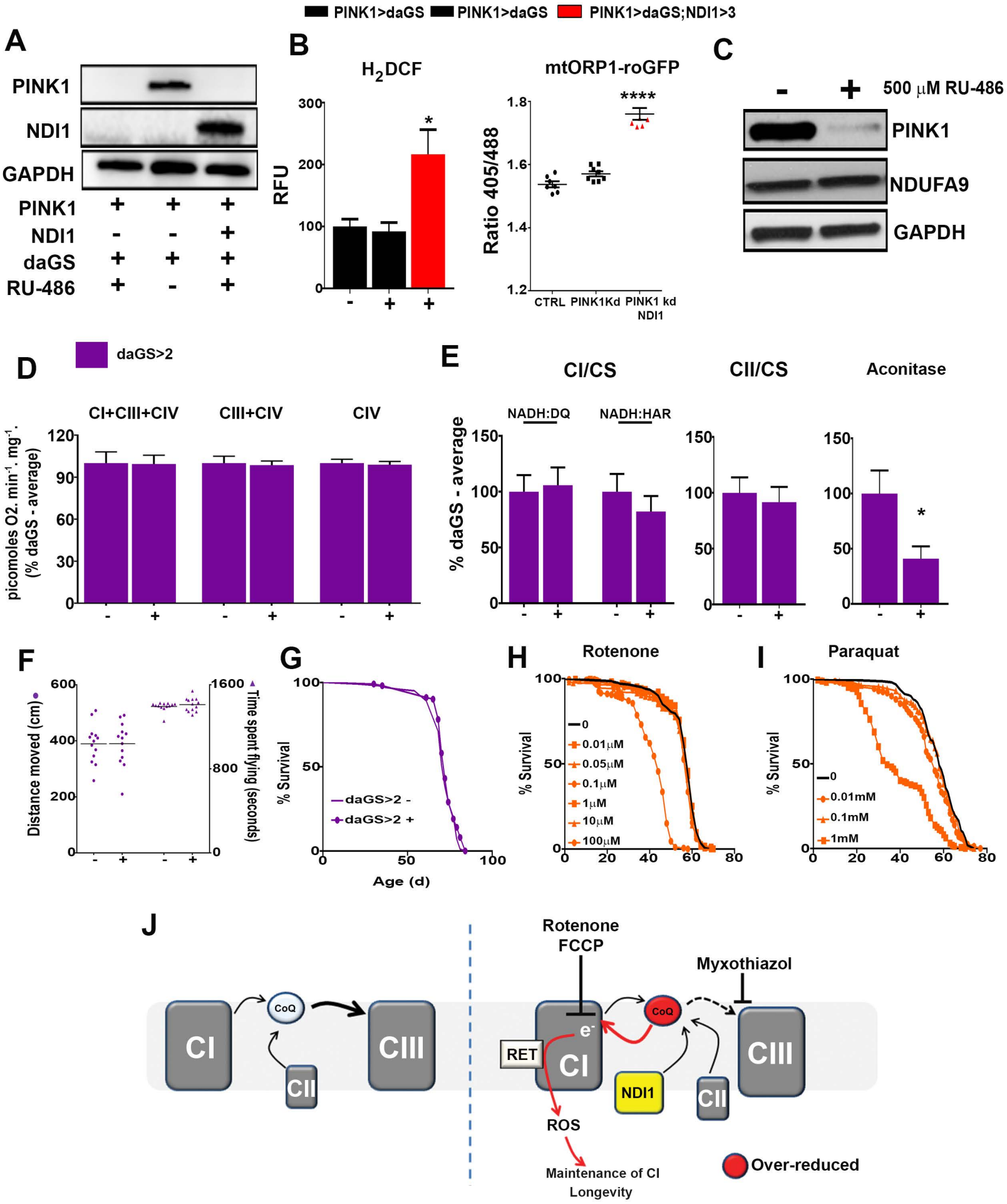

Scialò *et al.* Supplemental Figure 4

Supplemental Figure 4. Related to Figure 4. Preventing reduction of CoQ mediates age-related pathology.

(A) Representative western blots of PINK1 and NDI1 levels in the indicated genotypes.

(B) Quantification of fluorescence in brains dissected from flies from the indicated genotypes stained with H_2DCF (n=4) or expressing mtORP1-roGFP (n=4-8).

(C) Representative western blots of PINK1 and NDUFA9 levels in the indicated genotypes.

(D) Mitochondrial respiration in daGS>2 flies fed with RU-486 (+) and controls (-) (n=4).

(E) CI, CII and aconitase activities in daGS>2 flies fed with RU-486 (+) and controls (-) (n=4).

(F) Locomotive activity and flight time in daGS>2 flies fed with RU-486 (+) and controls (-) (n=13).

(G) Survival curves in daGS>2 flies fed with RU-486 (+) and controls (-) (n=200). See Table S1 for statistical analysis

(H) Survival curves of Dahomey flies fed with the indicated doses of rotenone (n=156-200). See Table S1 for statistical analysis.

(I) Survival curves of Dahomey flies fed with the indicated doses of paraquat (n=160). See Table S1 for statistical analysis.

(J) Model of NDI1-mediated extension of lifespan and maintenance of CI function. Black arrows indicate electron (e^-) transport events in forward direction; red arrows indicated e- transport events in reverse direction; flat-headed arrows indicate inhibition. Left, without NDI1; right, with NDI1.

Values shown represent means ± SEM of at least 3 biological replicates, unless otherwise stated. -/+ indicates presence/absence of 500 µM RU-486.

Table S1 -Related to Figures 2, 3 and 4 and Supplemental Figures 2, 3 and 4. Lifespan summary.

Statistical analysis of all lifespan experiments presented in this study. In parentheses, reference to the appropriate Figure panel is indicated.

NS indicates not significant differences.

Table S2. *Drosophila transgenic lines.* Related to Experimental Procedures.

Fly Strain	Source	Details
w^{Dah} *; UAS-Ndi1*	(Sanz et al., 2010)	Dahomey backcrossed UAS-Ndi1 on 3rd Chromosome
w^{Dah} *; UAS-AOX*	(Fernandez-Ayala et al., 2009)	Dahomey backcrossed UAS-AOX on 2nd Chromosome
w^{Dah} *; UAS-AOX*	(Fernandez-Ayala et al., 2009)	Dahomey backcrossed UAS-AOX on 3rd Chromosome
w^{Dah} *; UAS-SOD2*	Vienna Drosophila Resource Center (VDRC)	Dahomey backcrossed UAS-SOD2 RNAi on 2nd Chromosome (VDRC ID: 42162)
w^{Dah} *; UAS-ND-39*	VDRC	Dahomey backcrossed UAS-ND-39 (CI) RNAi on 2nd Chromosome (VDRC ID: 13131)
w^{Dah} *; UAS-levy*	VDRC	Dahomey backcrossed UAS-levy RNAi (CIV) on 2nd Chromosome (VDRC ID: 101523)
w^{Dah} *; UAS-Pink1*	VDRC	Dahomey backcrossed UAS-Pink1 RNAi on 2nd Chromosome (VDRC ID: 109614)
w^{Dah} *; daGAL4*	Bloomington *Drosophila* Stock Center (BDSC)	Dahomey backcrossed daughterless GAL4 driver on 3rd Chromosome (BDSC N^{o}: 55849)
w^{Dah}*; daGS*	(Tricoire et al., 2009)	Dahomey backcrossed daughterless GeneSwitch GAL4 driver on 2nd Chromosome
w^{Dah}*; actGS*	BDSC	Dahomey backcrossed Actin5c GeneSwitch GAL4 driver on 3rd Chromosome (BDSC N^{o}: 9431)
w^{Dah}*; UAS- mito-ORP1-roGFP2*	(Albrecht et al., 2011)	Dahomey backcrossed mitochondrially targeted ROS reporter on 2nd Chromosome
w^{Dah}*; UAS-mtCatalase*	(Mockett et al., 2010)	Dahomey backcrossed mitochondrially targeted catalase on 2nd Chromosome

Description of all transgenic fly lines (including the final background) used in this study.

Supplemental Experimental Procedures

Fly husbandry. Following eclosion, flies were tipped to new food and allowed to mate for 24 hours before being sorted and collected using CO_2 anesthesia. Female flies were used in all experiments. Flies were maintained at a density of 20 flies/vial and transferred to new food every 2-3 days. For all lifespan experiments, at least 80 flies were used. Each experiment was repeated at least 2-4 times as indicated in Table S1. Wild-type *Dahomey* and *Oregor R* strains were obtained from the laboratory of Prof Howy Jacobs (University of Helsinki). UAS-NDI1 flies and UAS-AOX flies have been described previously by Sanz *et al*. (2010) and Fernandez-Ayala *et al*. (2009), respectively. Flies containing UAS-RNAi constructs against *CG8905* (SOD2), *CG6020* (ND-39/NDUFA9), *CG17280* (levy, complex IV subunit VIa) and PINK1 were obtained from the Vienna Drosophila RNAi stock center (VDRC). Daughterless-GAL4 (daGAL4) and Actin-GeneSwitch-GAL4 (ActGS) flies were obtained from Bloomington Drosophila Stock Center. Daughterless-GeneSwitch-GAL4 (daGS) flies were a kind gift from Dr. Veronique Monnier (University of Paris). mito-ORP1-roGFP2 (mtORP1-roGFP) flies were a gift from Dr. Tobias Dick (German Cancer Research Center, Heidelberg). Mitochondrially targeted catalase (mtCAT) flies were a gift from Prof Rajindar Sohal. See Table S2 for details of the different fly strains used in this study. SOD2 RNAi expressing flies, CI>2;NDI1>daGAL4 flies, AOX>2;NDI1>daGAL4 flies, mtCAT>2;NDI1>daGAL4 flies and CIV>2;AOX>daGAL4 flies with respective controls were allowed to developed at 18^{o}C before being aged in 25^{o}C post-eclosion to reduce lethality in the experimental group during development. All strains and balancers used were backcrossed for a minimum of 6 generations to our white-eyed Dahomey background, derived from backcrossing the w^{1118} mutation into Dahomey for 11 generations. Dahomey virgin females were first crossed with males of each strain to ensure that all lines carried the same mitochondrial DNA. Virgin females from the F_1 generation were mated with Dahomey males and this cross was repeated for a minimum of six generations. Experimental flies were obtained by crossing females homozygous for the appropriate Gal4 driver (e.g. daGAL4>daGAL4) with males homozygous for one (e.g. NDI1>NDI1) or more transgenes (e.g. AOX>AOX;NDI1>NDI1). The experimental progeny carried one copy of the appropriate Gal4 driver and one copy of the desired transgene (e.g. AOX>2;NDI1>daGAL4). The only exception to this, was SOD2>CI;NDI1>ActGS flies (and controls for this experiment) that were produced by crossing virgin females carrying two copies of a UAS-SOD2 RNAi construct and one copy of the ActGS driver (SOD2>SOD2;ActGS>CyO) with either males homozygous for NDI1 (NDI1>NDI1) or males homozygous for NDI1 and heterozygous for a UAS-RNAi construct against ND-39 (CI>CyO;NDI1>NDI1). Flies containing more than two transgenes (e.g. AOX>AOX;NDI1>NDI1) were generated from backcrossed strains. Following backcrossing to Dahomey , flies homozygous for single

transgenes of interest were crossed to flies carrying balancers for the second and third chromosomes (CyO>2;TM3, $Sb^{[1]}$>3), as all the transgenes (Gal4/GS, UAS-cDNA or UAS-RNAi) we are working with are located on either 2nd or 3rd chromosomes. These balancer flies are regularly rederived to avoid accumulation of mutations. The progeny (e.g. F_1 UAS-X>CyO;TM3, $Sb^{[1]}$>3 or CyO>2;TM3, UAS-Y>$Sb^{[1]}$) were crossed to produce flies homozygous for a single transgene and heterozygous for a balancer (F_2 UAS-X>UAS-X; TM3, $Sb^{[1]}$>3 or CyO>2;TM3, UAS-Y>UAS-Y). In order to combine two transgenes, flies homozygous for single transgenes and heterozygous for a balancer (F_2) were crossed to generate flies with one copy of each transgene and each balancer (e.g. UAS-X>CyO; UAS-Y>TM3, $Sb^{[1]}$). These flies were then crossed together to generate flies homozygous for both constructs (eg UAS-X>UAS-X; UAS-Y>UAS-Y). Flies carrying single transgenes (e.g. daGal4, daGS, NDI1, AOX flies or UAS-CG2060 RNAi) were derived from the same crossing scheme in order to prevent background differences that can affect lifespan studies. Finally, transgene expression in experimental flies was confirmed by western blot or qPCR when antibodies were not available. To induce transgene expression in flies using GS drivers (i.e. daGS or i.e ActGS), food was supplemented with 300 or 500 μM RU-486. Food supplemented with rotenone (ROT; CI Q-site inhibitor), carbonyl cyanide-p-trifluoromethoxyphenylhydrazone (FCCP; uncoupler) or myxothiazol (MYX; CIII Q_o-site inhibitor) was prepared by adding 5 mM stock solutions in absolute EtOH to 2 ml of fly food to produce the desired concentrations. Food supplemented with paraquat was prepared by adding 2.5 mM stock solution in H_2O to 2 ml of fly food to the desired concentration. Control food was supplemented with EtOH or H_2O (vehicle) alone.

Isolation of crude mitochondrial fractions. All steps were performed at 4°C. 20-40 flies were homogenized in mitochondrial isolation buffer (MIB; 250 mM sucrose, 2 mM EGTA, 0.1% (w/v) bovine serum albumin (BSA), 5 mM tris-HCl pH 7.4) and filtered through 200μM netting. Following centrifugation at 200 x g, the supernatant was collected and centrifuged a second time at 9,000 x g. The mitochondrial pellet was resuspended in MIB without BSA. Mitochondria were used immediately for blue-native gel electrophoresis.

Blue-native gel electrophoresis (BNGE). 100 μg isolated mitochondria prepared as described above were pelleted and resuspended in 25 μl sample buffer (50 mM BisTris, 6N HCl, 50 mM NaCl, 10% w/v Glycerol, 0.001% Ponceau S, 1% w/v digitonin, supplemented with protease inhibitor cocktail (Roche)). Following a 15 minute incubation on ice, samples were centrifuged at max speed and the supernatant containing solubilized inner membrane complexes was collected

and supplemented with 10 µl sample buffer without digitonin and 1.5 µl PageBlue protein staining solution (ThermoFisher Scientific). 15 µl sample was then run on Novex Bis-Tris pre-cast gels and stained according to (Sanz et al., 2010).

Behavioral and locomotive activity assays. Individual flies were placed into empty vials. Live tracking of the flies was performed using a high-sensitivity The Imaging Source USB camera (equipped with a Computar 1/3" Varifocal Lens (2.8-12mm)), for 60 minutes per individual experiment. The recorded video files were saved and used to calculate distance moved per hour for each fly using the EthoVision XT video tracking software (Noldus Information Technology). Each video file was quantified at least two times (two replicates per individual fly). The distance moved was measured in centimeters and tabulated as centimeters/hour. The flying time of the individual fruit flies was calculated by manual set scoring using an inbuilt software timer. A 60 minute video recording was also used for this purpose. During manual scoring two behaviors, namely flying time and non-flying time were measured. This was repeated twice for each video file. The flying time was calculated in seconds and tabulated.

ROS detection. MitoSOX and dichlorofluorescein (H_2DCF) were used to measure either mitochondrial matrix superoxide or total cellular ROS levels, respectively, in adult fly brains dissected in PBS. Following dissection, fly brains were incubated in either 30 µM MitoSOX or 30 µM H_2DCF for 10 minutes before being washed 3 times with PBS and imaged immediately. Images were acquired using an LSM510 confocal microscope (Zeiss) equipped with a 10x 0.3 NA objective as Z stacks throughout the sample, using multi-line Argon laser. For *in vivo* ROS imaging using mtORP1-roGFP reporter lines, whole flies containing the reporter and driver, along with any other indicated constructs were put to sleep on ice before being dissected and imaged under Ex. 488 (reduced) or 405 (oxidized) nm/Em. 510 nm. The total (average) intensity of each individual brain imaged was quantified using ImageJ.

Electron microscopy. Dorsal flight muscles were dissected from flies of the indicated genotypes and indicated ages suspended in 0.16 M sym-collidine buffer pH 7.4 (Electron Microscopy Sciences) supplemented with 5% glutaraldehyde (fixing solution). Dissected muscles were maintained at 4^{o}C in fixing solution for at least 3 hours before undergoing osmium tetroxide (OsO_4) postfixation, followed by dehydration, embedding, sectioning and imaging according to (Ban-Ishihara et al., 2013). Muscle sections were imaged using a JEOL JEM-1400 Plus transmission electron microscope with attached 11 Mpx Olympus Quemesa digital camera. For quantification of size and circularity in SOD2 knockdown models, the mitochondria were

separated from the rest of the image by thresholding. The resulting thresholded binary image was then segmented using ImageJ watersheding algorithm (http://rsb.info.nih.gov/ij/plugins/watershed.html). The resulting segmented image was then used as an input for the particle analysis tool of ImageJ (http://rsbweb.nih.gov/ij/docs/guide/146-30.html). From the results table, the area and circularity (http://rsb.info.nih.gov/ij/plugins/circularity.html) distributions were plotted. For wild type Dahomey flies of different ages the images were manually segmented using GIMP (http://www.gimp.org/). The resulting segmented image was then again used as an input for the ImageJ particle analysis tool.

High-resolution respirometry. Whole-fly homogenates were used for respirometry measurements. Briefly, 20-40 flies were homogenized in MIB without BSA and filtered before being immediately measured using an OROBOROS O2k oxygraph. Homogenates were incubated in assay buffer (120 mM KCl, 5 mM KH_2PO_4, 3 mM Hepes, 1 mM EGTA, 1 mM $MgCl_2$, 0.2% bovine serum albumin, pH 7.2 at 25°C). State 4 respiration was initiated by addition of 5 mM pyruvate and 5 mM proline. State 3 was initiated with the addition of 1 mM ADP. CI-linked respiration (CI+CIII+CIV in figures) was inhibited adding 0.5 µM rotenone and 20 mM glycerol 3-phosphate was added to stimulate CIII-linked respiration (CIII+CIV in figures). CIII-linked respiration was inhibited with the addition of 2.5 µM antimycin A. CIV respiration (CIV in figures) was initiated by addition of 4 mM ascorbate and 2 mM TMPD. CIV respiration was inhibited by adding 0.5 mM KCN. Data presented corresponded to state 3 respiration (i.e.after ADP addition). Values were normalized to protein concentration as calculated by the Bradford method. Samples were flash frozen in liquid nitrogen and stored at -80^{o}C prior to use in subsequent enzymatic assays.

Enzymatic assays. All assays were adapted for use in a 96-well plate with a final volume of 300 µl using either a PerkinElmer EnVision 2104 (PerkinElmer) or a Fluostar Omega (BMG Labtech) plate reader. For ETC and citrate synthase assays, homogenates used in respirometry were thawed on ice and protein concentration was calculated via the Bradford method. CI activity was measured as rotenone-sensitive NADH dehydrogenase activity. 30 µl homogenate was added to 264 µl assay buffer consisting of 50 mM KH_2PO_4 pH 7.6, 3.5 mg/ml BSA and 50 µM decylubiquinone (DQ). The reaction was started with the addition of 6 µl 10 mM NADH and the decrease in absorbance at 340 nm was measured for 3 minutes at 25^{o}C. Rotenone-insensitive activity was followed for another 3 minutes following the addition of 1 µl 1 mM rotenone. Non-physiological activity through the matrix arm of CI was measured as

NADH:hexaammineruthenium chloride (HAR) oxidoreductase activity. Following addition of rotenone to inhibit CoQ/DQ-dependent activity, 6 µl 10 mM NADH and 7.5 µl 10 mM HAR were added and the decrease in absorbance at 340 nm was measured for 3 minutes at 25^{o}C. CIII activity (antimycin-sensitive decylubiquinol:cytochrome c oxidoreductase) was measured according to the optimized method used by (Luo et al., 2008). Complex II (CII), IV and V activities were measured according to (Barrientos, 2002) with slight modifications. Briefly, CII activity (malonate-sensitive succinate:dichlorophenolindophenol (DCPIP) oxidoreductase) was measured by adding 40 µl of homogenate to 258 µl of assay buffer (10 mM KH_2PO_4 pH 7.6, 1 mg/ml BSA, 2 mM EDTA, 80 µM DCPIP, 4 µM rotenone, 10 mM succinate, 0.2 mM ATP). Following 10 minutes of pre-incubation at 25°C to allow succinate to overcome the inhibitory effect of oxaloacetate, 2 µl of 1.55 mM decylubiquinone was added to initiate the reaction and the decrease in absorbance at 600 nm was measured for 3 minutes. Non-CII activity was discarded by the addition of 2 µl 1 M malonate. CIV activity (potassium cyanide-sensitive cytochrome c oxidase) was measured by resuspending 30 µl fly homogenate in 210 µl assay buffer (10 mM KH_2PO_4 pH 6.5, 250 mM sucrose, 1 mg/ml BSA). The reaction was initiated by the addition of 60 µl 0.22 mM reduced cytochrome c (0.22 mM cytochrome c solution supplemented with 0.5 mM DTT and incubated at room temperature for 15 minutes) and the decrease in absorbance was measured at 550 nm for 3 minutes before being supplemented with 2 µl 0.1 M KCN and measured again. Complex V activity (oligomycin-sensitive NADH-coupled ATPase activity) by resuspending 20 µl homogenate in 243 µl assay buffer (50 mM Tris pH 8, 5 mg/ml BSA, 20 mM $MgCl_2$, 50 mM KCl). The reaction was initiated by the addition of 37 µl of initiation mix (24.3 µM FCCP, 8.1 µM Antimycin A, 4.05 mM ATP, 109 U/ml Lactate dehydrogenase, 108 U/ml pyruvate kinase, 2.43 mM NADH and 24.3 mM phosphoenolpyruvate) and the decrease in absorbance at 340 nm was measured for 3 minutes. 2 µl 0.5 mg/ml oligomycin was added to each well and the rate was measured again. All ETC activities were normalized to mitochondrial density calculated by citrate synthase (CS) activity measured according to (Magwere et al., 2006). Whole and mitochondrial fractions of fly homogenates were supplemented with 1 mM dithiothreitol and 1 mM phenylmethylsulfonyl fluoride before use in CS activity assay. Mitochondrial aconitase activity was measured as in (Muller et al., 2004) with a few modifications. Mitochondria (0.01 mg/ml) were pre-incubated in assay buffer (50 mM KH_2PO_4 (pH 7.4), 0.6 mM $MgCl_2$, 5 mM sodium citrate, 0.2 mM $NADP^+$, 0.4 U/ml Isocitrate dehydrogenase ($NADP^+$)). The assay was initiated by permeabilisation of mitochondrial membranes with the addition of 0.01% Triton X-100. Activity was measured at 25^{o}C using a PerkinElmer EnVision 2104 plate reader at 355 nm/460 nm Ex./Em. for 30 minutes. Non-specific activity (assay without isocitrate dehydrogenase) was subtracted from final values.

Western blots. All sample preparation steps were performed at 4^{o}C as described in (Fernandez-Ayala et al., 2009). Protein concentration was calculated by the Bradford method before loading into pre-cast AnykD Criterion TGX Stain-Free (BIO-RAD) polyacrylamide gels for electrophoresis. Following electrophoresis, proteins were blotted onto Hybond nitrocellulose membranes and blocked with 5% milk in PBS-Tween 20 for 1 hour at room temperature before being probed overnight at 4^{o}C with the indicated antibodies diluted in 5% milk in PBS-Tween 20. Antibody dilutions are as follows: NDUFS3 (Abcam), 1:10,000; Aconitase 2 (Abcam), 1: 2,000; PARKIN (Sigma-Aldrich), 1:2,000; PINK1 (Sigma-Aldrich), 1:500; GAPDH (Everest Biotech), 1:30,000; SDHB (Abcam), 1:250; COXIV (Abcam), 1:7,500; Cytochrome b (Abmart), 1:1,000; ATP5A (Abcam), 1:500,000; SOD2 (Abcam), 1:1,000; NDUFA8 and NDUFA9 (A gift from Prof Howy Jacobs (University of Helsinki)), 1:1,000 and 1:2,500 respectively; NDI1 (a gift from the lab of Prof Takao Yagi (Scripps)) 1:10,000; AOX (a gift from the lab of Prof Howy Jacobs (University of Helsinki)), 1:20,000; Catalase (GeneTex), 1:1,000.

CAFÉ assay to measure food intake. Glass capillaries containing CAFÉ assay food (5% sucrose and 5% yeast extract) were inserted into the tops of 1.5 ml tubes (1 per tube). Another hole was made in the tube to allow air circulation. Flies were anesthetized with CO_2 and transferred to the tube. Quantification of food intake was performed by adding a known amount of food into the capillaries, and then measuring changes in this volume every 24 hours. Food evaporation was controlled for by measuring capillaries in tubes without flies. The analysis was carried out for around 120 hours.

RNA quantification. The methods for the isolation of mRNA and cDNA synthesis and q-RT-PCR analysis have been described in detail in (Sanz et al., 2010). The data were extracted and analysed using Applied Biosystems StepOne software version 2.1. Primer sequences are available upon request.

Measurement of redox state of CoQ. 20 frozen flies were homogenized according to (Sanz et al., 2010). A single sample was processed each time to prevent artificial oxidation of ubiquinol. Lipids were extracted by adding 300 µl of 2-propanol and 1:1000 beta-mercaptoethanol to 100 µl of fly homogenate. Samples were centrifuged at 16,000 x g for 1 minute at 4 ºC and 100 µl of the supernatant was immediately injected into a 166-126 HPLC system (Beckman-Coulter) equipped with an UV/Vis detector (System Gold R 168, Beckman-Coulter) and an electrochemical

(Coulochem III ESA) detector. Separation was carried out in a 15 cm Kromasil C18 column (Scharlab, Spain) at 40ºC with a mobile phase of methanol/n-propanol (65:35) containing 1.42 mM lithium perclorate at a flow-rate of 1 ml/min. UV-spectrum was used to identify the different forms of ubiquinone (oxidized CoQ9 and CoQ10 with maximum absorption at 275 nm) and ubiquinol (reduced CoQ, CoQ9H2 and CoQ10H2, with maximum absorption at 290 nm) using specific standards, and the electrochemical readings were used for their quantification. Redox status of CoQ was calculated as follows:

% reduced CoQ = (CoQ9H2+CoQ10H2)/(CoQ9H2+CoQ10H2+CoQ9+CoQ10).

Statistical analysis. Values shown represent means ± SEM. $p<0.05$ was taken as statistically significant. Data were analyzed with Prism 6 (GraphPad) using either 1-way ANOVA with Newman-Keul's post-test or using the unpaired Student's t-test where appropriate. Lifespan data were analyzed using the log-rank Mantel Cox Test. Different symbols in graphs denote significantly different groups ($p<0.05$). * = $p<0.05$; ** = $p<0.01$; *** = $p<0.005$; **** = $p<0.001$ indicate significant difference from all other groups unless indicated otherwise by line art. NS = not significantly different. Individual and combined lifespan experiments with statistical analysis are summarized in Table S1.

Supplemental References

Albrecht, S.C., Barata, A.G., Großhans, J., Teleman, A.A., and Dick, T.P. (2011). In Vivo Mapping of Hydrogen Peroxide and Oxidized Glutathione Reveals Chemical and Regional Specificity of Redox Homeostasis. Cell metabolism *14*, 819-829.

Ban-Ishihara, R., Ishihara, T., Sasaki, N., Mihara, K., and Ishihara, N. (2013). Dynamics of nucleoid structure regulated by mitochondrial fission contributes to cristae reformation and release of cytochrome c. Proc Natl Acad Sci U S A *110*, 11863-11868.

Barrientos, A. (2002). In vivo and in organello assessment of OXPHOS activities. Methods *26*, 307-316.

Fernandez-Ayala, D.J., Sanz, A., Vartiainen, S., Kemppainen, K.K., Babusiak, M., Mustalahti, E., Costa, R., Tuomela, T., Zeviani, M., Chung, J., *et al.* (2009). Expression of the Ciona intestinalis alternative oxidase (AOX) in Drosophila complements defects in mitochondrial oxidative phosphorylation. Cell Metab *9*, 449-460.

Luo, C., Long, J., and Liu, J. (2008). An improved spectrophotometric method for a more specific and accurate assay of mitochondrial complex III activity. Clin Chim Acta *395*, 38-41.

Magwere, T., Pamplona, R., Miwa, S., Martinez-Diaz, P., Portero-Otin, M., Brand, M.D., and Partridge, L. (2006). Flight activity, mortality rates, and lipoxidative damage in Drosophila. J Gerontol A Biol Sci Med Sci *61*, 136-145.

Mockett, R.J., Sohal, B.H., and Sohal, R.S. (2010). Expression of multiple copies of mitochondrially targeted catalase or genomic Mn superoxide dismutase transgenes does not extend the life span of Drosophila melanogaster. Free Radic Biol Med *49*, 2028-2031.

Muller, F.L., Liu, Y., and Van Remmen, H. (2004). Complex III releases superoxide to both sides of the inner mitochondrial membrane. J Biol Chem *279*, 49064-49073.
Sanz, A., Soikkeli, M., Portero-Otin, M., Wilson, A., Kemppainen, E., McIlroy, G., Ellila, S., Kemppainen, K.K., Tuomela, T., Lakanmaa, M., *et al.* (2010). Expression of the yeast NADH dehydrogenase Ndi1 in Drosophila confers increased lifespan independently of dietary restriction. Proc Natl Acad Sci U S A *107*, 9105-9110.
Tricoire, H., Battisti, V., Trannoy, S., Lasbleiz, C., Pret, A.M., and Monnier, V. (2009). The steroid hormone receptor EcR finely modulates Drosophila lifespan during adulthood in a sex-specific manner. Mechanisms of ageing and development *130*, 547-552.